

Muon Identification without Iron

John Hauptman *

Iowa State University, Department of Physics and Astronomy
Ames, IA 50011 USA

Muons can be identified with high efficiency and purity and reconstructed with high precision in a detector with a dual readout calorimeter and a dual solenoid to return the flux without iron. We show CERN test beam data for the calorimeter and calculations for the magnetic fields and the track reconstruction. For isolated tracks, the rejection of pions against muons ranges from 10^3 at 20 GeV/c to 10^5 at 300 GeV/c.

1 Introduction

Big detectors at high energy colliders require the detection of electrons (e) and muons (μ) with high efficiency, high purity and high precision for the reconstruction of the decays $W \rightarrow e\nu$, $W \rightarrow \mu\nu$, $Z \rightarrow e^+e^-$, $Z \rightarrow \mu^+\mu^-$, for the identification of τ lepton decays to e and μ , for searches for lepton number violation, for the positive tagging of events with missing neutrinos, and for the isolation of event samples with supposed decays of supersymmetric or other massive states decaying partly to leptons. The muon system of the 4th Concept, Fig. 1, achieves almost absolute muon identification for isolated tracks.

2 Separation of muons (μ^\pm) from charged pions (π^\pm)

We achieve excellent $\mu - \pi^\pm$ separation using three independent measurements: (a) energy balance from the tracker through the calorimeter into the muon spectrometer, (b) a unique separation of the radiative component from the ionization component in the dual-readout calorimeter; and, (c) a measurement of the neutron content in the dual-readout fiber calorimeter.

2.1 Separation energy and momentum balance

The central tracking system has a resolution of about $\sigma_p/p^2 \sim k_1$ ($k_1 \sim 3 \times 10^{-5} (\text{GeV}/c)^{-1}$) and the muons spectrometer in the annulus between the solenoids with

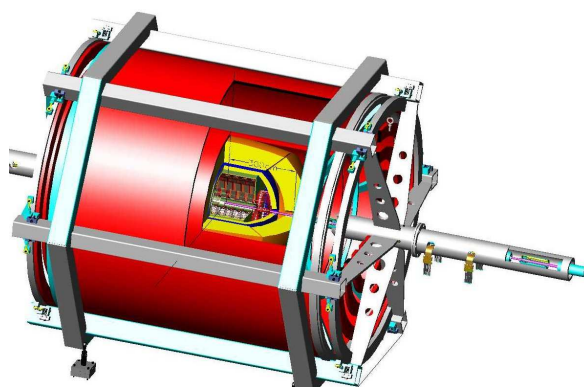


Figure 1: 4th Concept detector showing the dual solenoids. The annulus between the solenoids is filled with cluster counting wires inside precision tubes.

a B=1.5 T field has resolution of about $\sigma_p/p^2 \sim k_2$

*This work has been supported by the US Department of Energy through DE-FG02-91ER40634 and LCRD Project 6.18.

($k_2 \sim 5 \times 10^{-4} (\text{GeV}/c)^{-1}$). A muon of momentum p which radiates energy E in the volume of the calorimeter that is measured with a resolution of $\sigma_E/E \sim 0.20/\sqrt{E}$ will have a momentum-energy balance constraint of $[k_1 p^2 \oplus 0.2\sqrt{E} \oplus k_2(p - E)^2]/p$ which yields a rejection of about 30 for a 100 GeV muon radiating 20 GeV.

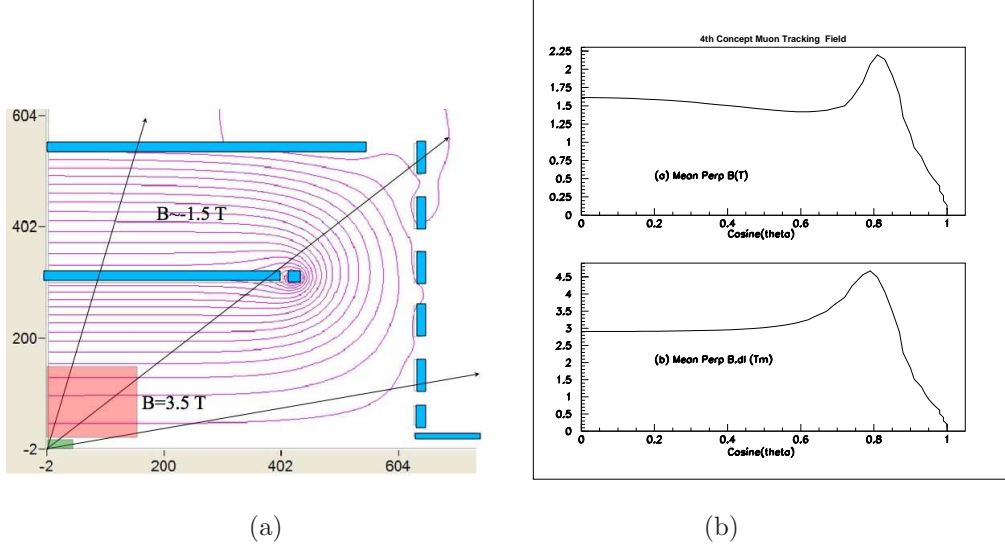


Figure 2: (a) The field map of the dual solenoids showing the wall of coils and the almost completely confined field; (b) the mean bending field (1.5 T) along muon trajectories from the origin and the integral of the mean bending field (3 Tm).

2.2 Separation by dual-readout

A non-radiating muon penetrating the mass of a fiber dual readout calorimeter will leave a signal in the scintillating fibers equivalent to the dE/dx of the muon, which in DREAM is about 1.1 GeV. There will be no Čerenkov signal since the Čerenkov angle is larger than the capture cone angle of the fiber. A radiating muon will add equal signals to both the scintillating and Čerenkov fibers and, therefore, the difference of the scintillating (S) and Čerenkov (C) signals is

$$S - C \approx \overline{dE/dx} \approx 1.1 \text{ GeV}$$

independent of the degree of radiation. The distributions of $(S - C)$ vs. $(S + C)/2$ for 20 GeV^a and 200 GeV π^- and μ^- are shown in Fig. 3 in which for an isolated track the π^\pm rejection against μ is about 10^3 at 20 GeV and 10^4 at 200 GeV. The distribution of $(S - C)$ as a mean that is very nearly 1.1 GeV as expected, and the radiative events are evident at larger $(S + C)/2$.

^aThere were no μ^- left in the H4 beam at 20 GeV/c, so these data are from 40 GeV/c μ^- .

2.3 Separation by neutron content measurement

The DREAM collaboration has succeeded in the measurement of neutron content in hadronic showers event-by-event in the DREAM module by summing the scintillating channels of the module in three radial rings and digitizing the PMT output at 1.25 GHz. These data, now being analyzed, show clearly the long-time neutron component in hadron showers that is absent in electromagnetic showers (and also absent in the Čerenkov fibers of the DREAM module for both e and π).

We expect to estimate a neutron fraction, f_n , each event the same way we estimate f_{EM} each event, and be able to reject localized hadronic activity in the calorimeter with factors of 10-50.

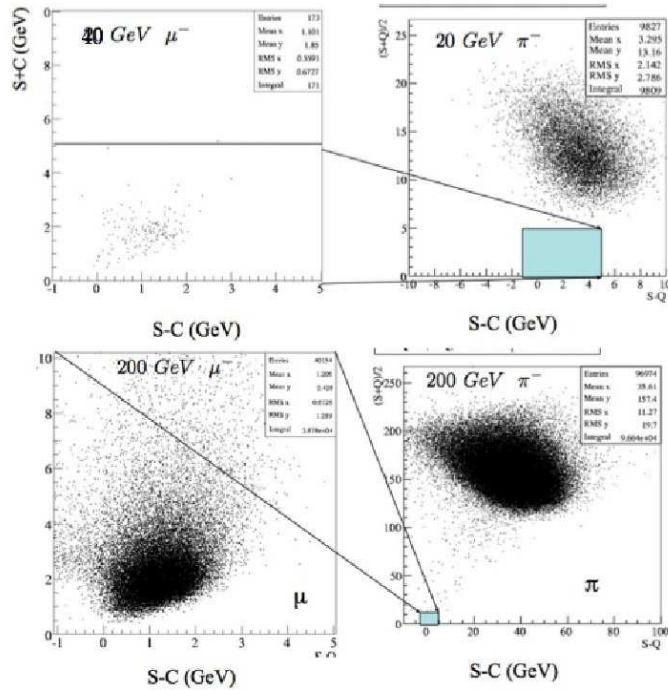


Figure 3: Dual-readout separation of $\mu - \pi^\pm$.

3 Summary

Any simple product of these three rejection factors, or any estimate of the muon efficiency and purity, gives an optimistic result that will clearly be limited by tracking efficiencies, overlapping shower debris in the calorimeter, or track confusion either in the main tracker or the muon spectrometer before these beam test numbers are reached. Nevertheless, we expect excellent muon identification.

References

- [1] Slides: <http://ilcagenda.linearcollider.org/contributionDisplay.py?contribId=377\&sessionId=108&confId=1296>
- [2] 4th Concept Detector Outline Document is available at the WWS-OC website <http://physics.uoregon.edu/lc/wwstudy/concepts/>.
- [3] "Muon Detection with a Dual-Readout Calorimeter", N. Akchurin, *et al.*, *Nucl. Instr. Meths. A* **533** (2004) 305-321.
- [4] "Electron Detection with a Dual-Readout Calorimeter", N. Akchurin, *et al.*, *Nucl. Instr. Meths. A* **536** (2005) 29-51.